Supporting Information

High-Performance Polybenzimidazole Membranes for Helium Extraction from Natural Gas

Xuerui Wang,*,† *Meixia Shan*,† *Xinlei Liu*,† *Meng Wang*,‡ *Cara M. Doherty*,§ *Dmitrii Osadchii*,† *Freek Kapteijn*,*,†

†Chemical Engineering Department, Delft University of Technology, Van der Maasweg 9, 2629 HZ Delft, The Netherlands

‡Process & Energy Department, Delft University of Technology, Leeghwaterstraat 39, 2628 CB DELFT, The Netherlands

§The Commonwealth Scientific and Industrial Research Organization (CSIRO) Manufacturing Private Bag 10, Clayton, South Victoria 3169, Australia

*Corresponding authors:

Xuerui Wang: x.wang-12@tudelft.nl

Freek Kapteijn: f.kapteijn@tudelft.nl

1

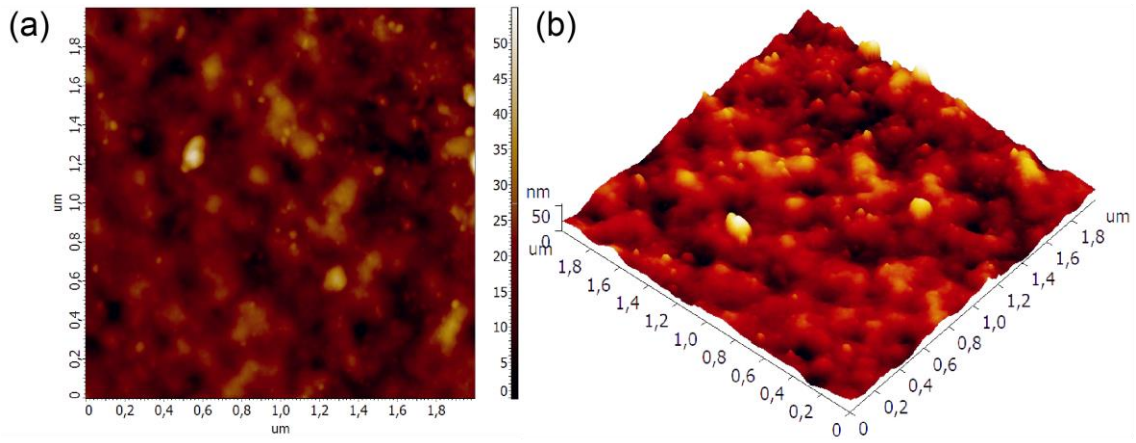

Figure S1 2D (a) and 3D (b) AFM image of PBDI membrane surface.

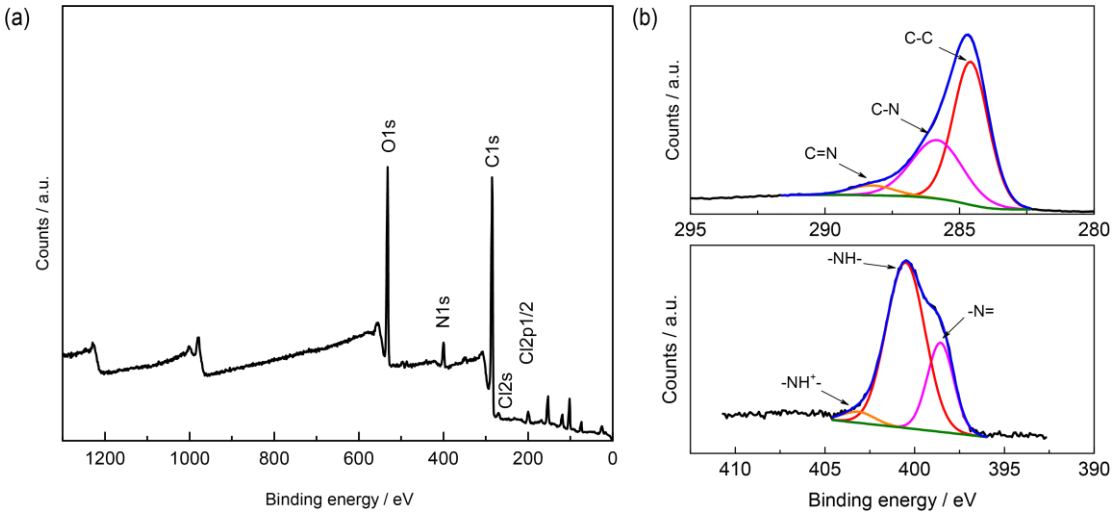

Figure S2 (a) XPS overview spectrum, (b) detail C_{1s} and N_{1s} spectra of the PBDI membrane.

The surface composition of the PBDI membrane was characterized by XPS (*Figure S2a*). The XPS spectrum shows peaks at 202, 270, 284, 399, and 532 eV, which are attributed to Cl_{2p}, Cl_{2s}, C_{1s}, N_{1s}, and O_{1s}, respectively. Chlorine residues, which stem from BTA, might be trapped within the membrane layer during interfacial polymerization. The C_{1s} spectrum deconvolution shows three peaks at 284.6, 285.9 and 288.3 eV (*Figure S2b*), which are attributed to the carbon atoms within phenyl groups, C-N, and C=N, respectively.[1] The deconvoluted N_{1s} spectrum shows three peaks at 398.6, 400.5 and 403.0 eV (*Figure S2b*), which are attributed to the –N=, -NH-, and $=NH^{+}$-, respectively.[1]

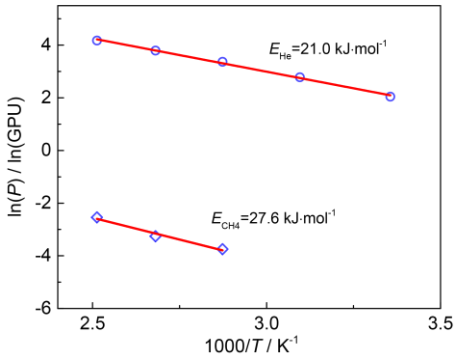

Figure S3 Arrhenius representation for the He and CH_4 permeance of the PBDI membrane for an equimolar He/CH_4 mixture at 1 bara feed pressure.

The CH_4 permeance was beyond the GC detection limit at relatively low temperature. The apparent permeation activation energies were determined by the Arrhenius relation:

$$\ln P_i = -\frac{E_{act,i}}{R}\frac{1}{T} + a \tag{4}$$

where $E_{act,i}$ is the apparent activation energy of component i, kJ mol^{-1}, R is the ideal gas constant, 8.314 J mol^{-1} K^{-1}, T is the absolute temperature, K.

In the Henry regime (linear adsorption), the apparent permeation activation energy can be envisaged as the sum of diffusivity activation energy (E_{diff}, positive value) and adsorption enthalpy (ΔH_{ads}, negative value).[2]

$$E_{act} = E_{diff} + \Delta H_{ads} \tag{5}$$

Because of the non-adsorbing property of He, its adsorption enthalpy can be considered as zero.[3] The adsorption enthalpy of CH_4 in benzimidazole-linked polymers is (-18.6)~(-21.7) kJ/mol.[4-5] Therefore, the diffusion activation energy is estimated to be 21.0 kJ mol^{-1} and 46.2 kJ mol^{-1} for He and CH_4, respectively, indicating an activated diffusion process for both He and CH_4.

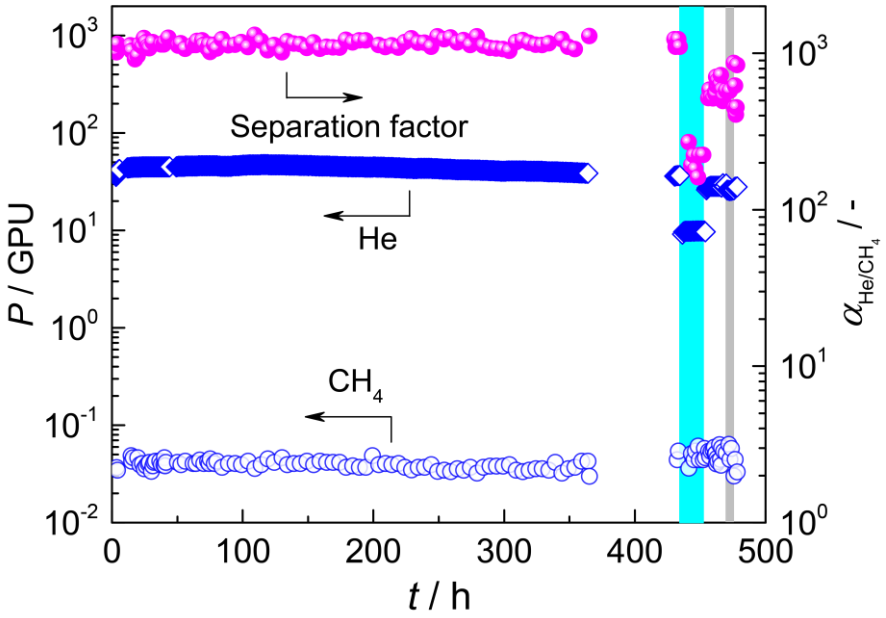

Figure S4 Long-term performance of PBDI membrane for He/CH_4 mixture separation, and effect of water vapour (3 kPa, *cyan shading*) and hydrocarbon (5 kPa *i*-butane, *gray shading*) addition. Operating conditions: 1 bara feed pressure and 100 °C, sweep gas argon.

The performance was constant for ~430 h in dry He/CH_4 mixture. Both He permeance and selectivity dropped significantly when water vapour was introduced. One reason is the competitive adsorption of H_2O by PBDI polymers, causing blockage of the pathway for He diffusion; the other reason is the reduced *d*-spacings of hydrated PBDI polymers due to the hydrogen bonding with nitrogen atoms.[6] Only 80% He permeance was recovered after cutting off the water vapour, indicating strong interaction between water and polymeric chains. In the presence of hydrocarbon contamination, He permeance decreased by 7% and it can be fully recovered by removal of the *i*-C_4. This phenomenon is attributed to the pore entrance blockage by adsorption of the hydrocarbon. This full recovery excludes any physical aging.

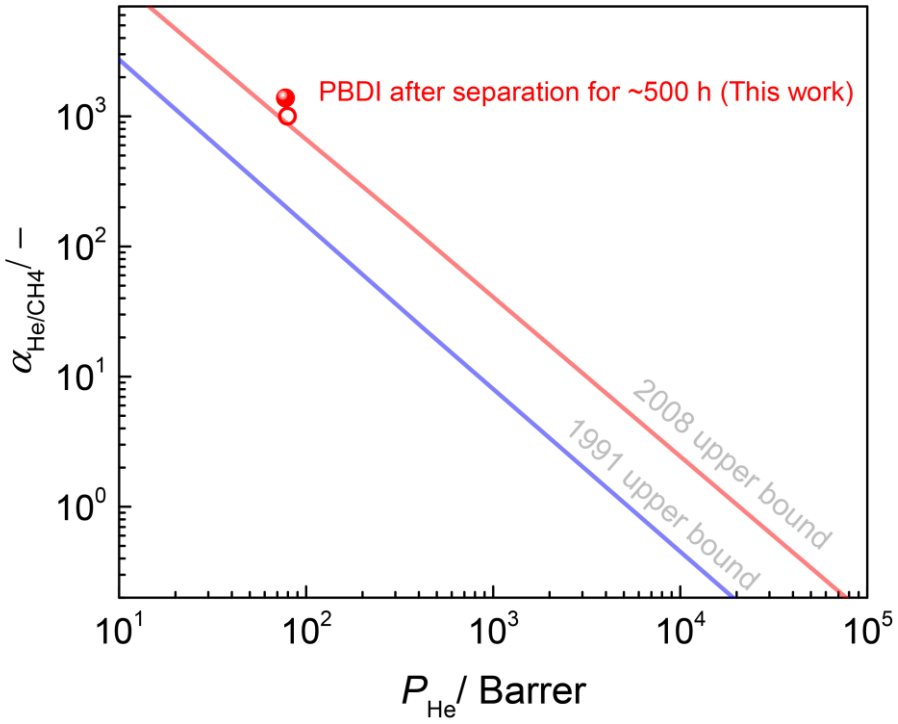

Figure S5 Comparison of PBDI membranes with the state of the art in He/CH_4 mixture separation in a Robeson-plot (selectivity versus permeability). The open and solid labels represent pure gas separation performance (ideal selectivity) and He/CH_4 mixture separation performance, respectively; the blue and red lines denote the 1991 and 2008 Robeson's upper bounds of polymeric membranes for He/CH_4 separation.[7]

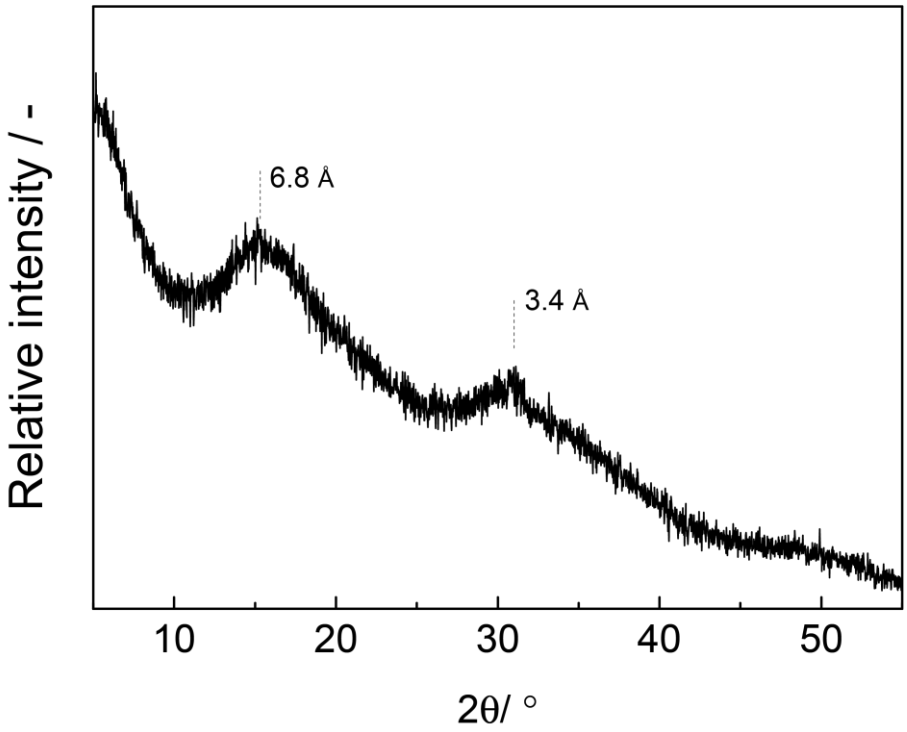

Figure S6 PXRD pattern of PBDI film species.

Table S1. He/CH_4 separation performance summary of PBDI membranes.

Number	Reaction time / h	P / *GPU*	α / –
M1	0.1	1500	1.9
M2	0.5	51	5.4
M3	1	34	400
M4	3	45	1380

The separation performance was tested in equimolar He/CH_4 mixture at 100 °C and 1 bara feed pressure, sweep gas Ar.

Table S2**.** The data points shown in Figure 4a for He/CH_4 separation.

Polymer	*Thickness* / μm	Feed	*T* / °*C*	*p* / *bara*	*P* / *GPU*	*S* / –	α / –	Ref
Hyflon AD60X	60.6	He or CH_4	25	1	5.9	11.6	N.A.	8
Hyflon AD60X	65.2	He or CH_4	25	1	7.3	157.1	N.A.	8
Hyflon AD60X	67.7	He or CH_4	25	1	5.0	16.9	N.A.	8
Hyflon AD60X	68.3	He or CH_4	25	1	6.7	136	N.A.	8
Hyflon AD60X	220	He or CH_4	25	1	1.8	167	N.A.	8-9
Hyflon AD60X	122	He or CH_4	25	1	3.0	32.9	N.A.	9-10
Hyflon AD60	0.2	He or CH_4	22	3.4	2600	35	N.A.	11
Hyflon AD60X	15~150	He or CH_4	25	1	22	36.7	N.A.	12
Hyflon AD80X	24.9	He or CH_4	25	1	11.6	47.4	N.A.	12
Cytop	0.2	He or CH_4	22	3.4	790	130	N.A.	11
Teflon AF 1600	15~150	He or CH_4	25	1	57.4	20.6	N.A.	12
Teflon AF 2400	15~150	He or CH_4	25	1	194	6.3	N.A.	12
Teflon AF 2400	20	He or CH_4	25	3.4	180	6	N.A.	13
Teflon AF 2400	0.16	He or CH_4	22	3.4	10500	4.6	N.A.	11
PBDI	1.73	He or CH_4	100	1	46	1000	N.A.	This
PBDI	1.73	50He/50CH_4	100	1	45	N.A.	1380	work

Table S3**.** Physical properties of PBDI and commercial perfluoropolymers.

Polymer	T_g / °C	*d*-spacing[a]/ Å	FFV	Free volume size[b]/ Å	Ref
Teflon AF 1600	162	9.1 (2.3)	0.31	4.5 & 10.1	14-15
Hyflon AD80	134	8.2 (4.0, 2.3)	0.23	10.4	14, 16
PBDI	N.A.	3.4, 6.8	N.A.	4.3[b]	This work

[a]: Values correspond to the main reflection and the minor reflection (in parentheses) as shown in *Figure S6*; [b]: Determined by positron annihilation lifetime spectroscopy (PALS).

Table S4**.** He/CO_2 separation performance comparison between PBDI and perfluoropolymer membranes.

Polymer	*Thickness* / μm	Feed	T / °C	p / *bara*	P_{He} / *GPU*	P_{CO_2} / *GPU*	Ref
Teflon AF 2400	0.2	He or CO_2	22	3.4	10500	13000	11
Hyflon AD60	0.2	He or CO_2	22	3.4	2600	1300	11
Cytop	0.2	He or CO_2	22	3.4	790	150	11
PBDI	1.73	He or CO_2	100	1	46	0.98	This work

References

(1) Liu, S.; Tian, J.; Wang, L.; Zhang, Y.; Qin, X.; Luo, Y.; Asiri, A. M.; Al-Youbi, A. O.; Sun, X., Hydrothermal Treatment of Grass: A Low-Cost, Green Route to Nitrogen-Doped, Carbon-Rich, Photoluminescent Polymer Nanodots as an Effective Fluorescent Sensing Platform for Label-Free Detection of Cu(II) Ions. *Adv Mater,* **2012**, *24*, 2037-2041.

(2) Kapteijn, F.; van de Graaf, J. M.; Moulijn, J. A., One-Component Permeation Maximum: Diagnostic Tool for Silicalite-1 Membranes? *AIChE J,* **2000**, *46*, 1096-1100.

(3) Gumma, S.; Talu, O., Gibbs Dividing Surface and Helium Adsorption. *Adsorption,* **2003**, *9*, 17-28.

(4) Sekizkardes, A. K.; İslamoğlu, T.; Kahveci, Z.; El-Kaderi, H. M., Application of Pyrene-Derived Benzimidazole-Linked Polymers to CO_2 Separation under Pressure and Vacuum Swing Adsorption Settings. *J Mater Chem A,* **2014**, *2*, 12492-12500.

(5) Rabbani, M. G.; El-Kaderi, H. M., Template-Free Synthesis of a Highly Porous Benzimidazole-Linked Polymer for CO_2 Capture and H_2 Storage. *Chem Mater,* **2011**, *23*, 1650-1653.

(6) Li, S.; Fried, J. R.; Colebrook, J.; Burkhardt, J., Molecular Simulations of Neat, Hydrated, and Phosphoric Acid-Doped Polybenzimidazoles. Part 1: Poly(2,2′-*M*-Phenylene-5,5′-Bibenzimidazole) (PBI), Poly(2,5-Benzimidazole) (ABPBI), and Poly(*P*-Phenylene Benzobisimidazole) (PBDI). *Polymer,* **2010**, *51*, 5640-5648.

(7) Robeson, L. M., The Upper Bound Revisited. *J Membr Sci,* **2008**, *320*, 390-400.

(8) Macchione, M.; Jansen, J. C.; De Luca, G.; Tocci, E.; Longeri, M.; Drioli, E., Experimental Analysis and Simulation of the Gas Transport in Dense Hyflon® AD60X Membranes: Influence of Residual Solvent. *Polymer,* **2007**, *48*, 2619-2635.

(9) Jansen, J. C.; Macchione, M.; Drioli, E., On the Unusual Solvent Retention and the Effect on the Gas Transport in Perfluorinated Hyflon AD® Membranes. *J Membr Sci,* **2007**, *287*, 132-137.

(10) Jansen, J. C.; Tasselli, F.; Tocci, E.; Drioli, E., High-Flux Composite Perfluorinated Gas Separation Membranes of Hyflon® AD on a Hollow Fibre Ultrafiltration Membrane Support. *Desalination,* **2006**, *192*, 207-213.

(11) Okamoto, Y.; Zhang, H.; Mikes, F.; Koike, Y.; He, Z.; Merkel, T. C., New Perfluoro-Dioxolane-Based Membranes for Gas Separations. *J Membr Sci,* **2014**, *471*, 412-419.

(12) Jansen, J. C.; Friess, K.; Drioli, E., Organic Vapour Transport in Glassy Perfluoropolymer Membranes: A Simple Semi-Quantitative Approach to Analyze Clustering Phenomena by Time Lag Measurements. *J Membr Sci,* **2011**, *367*, 141-151.

(13) Pinnau, I.; Toy, L. G., Gas and Vapor Transport Properties of Amorphous Perfluorinated Copolymer Membranes Based on

2,2-Bistrifluoromethyl-4,5-Difluoro-1,3-Dioxole/Tetrafluoroethylene. *J Membr Sci*, **1996**, *109*, 125-133.

(14) Yavari, M.; Fang, M.; Nguyen, H.; Merkel, T. C.; Lin, H.; Okamoto, Y., Dioxolane-Based Perfluoropolymers with Superior Membrane Gas Separation Properties. *Macromolecules*, **2018**, *51*, 2489-2497.

(15) Rudel, M.; Kruse, J.; Rätzke, K.; Faupel, F.; Yampolskii, Y. P.; Shantarovich, V. P.; Dlubek, G., Temperature Dependence of Positron Annihilation Lifetimes in High Permeability Polymers: Amorphous Teflons AF. *Macromolecules*, **2008**, *41*, 788-795.

(16) Jansen, J. C.; Macchione, M.; Tocci, E.; De Lorenzo, L.; Yampolskii, Y. P.; Sanfirova, O.; Shantarovich, V. P.; Heuchel, M.; Hofmann, D.; Drioli, E., Comparative Study of Different Probing Techniques for the Analysis of the Free Volume Distribution in Amorphous Glassy Perfluoropolymers. *Macromolecules*, **2009**, *42*, 7589-7604.